Low-field electron runaway and spontaneous formation of two-beam velocity distribution in polar semiconductors

S. M. Komirenko and K. W. Kim*
Department of Electrical and Computer Engineering, North Carolina State University, Raleigh, North Carolina 27695-7911, USA

V. A. Kochelap
Institute of Semiconductor Physics, National Academy of Sciences, Kiev, 252650, Ukraine

D. L. Woolard
Electronics Division, US Army Research Office, Research Triangle Park, North Carolina 27709, USA
(Received 3 June 2003; revised manuscript received 15 September 2003; published 10 June 2004)

We show that high-energy electron injection into a polar semiconductor can lead to a spontaneous splitting of the electron beam into two distinct groups with different velocity distributions. While one group of electrons experiences *thermalization* in a given subthreshold field, the velocity and energy of the second group increases with distance due to the previously unknown low-field electron runaway effect. We investigate the dependence of the carrier distribution on the injection energy, and show that the overall distribution exhibits a partial population inversion with a distance-dependent energy gap between the thermalized and runaway electrons. The low-field runaway is a universal effect which is characteristic of nanoscale semiconductors where polar optical phonon scattering predominates and there is a large intervalley energy separation as in the group-III nitride heterostructures.

DOI: 10.1103/PhysRevB.69.233201 PACS number(s): 72.20.Ht, 72.10.Di, 72.80.Ey, 72.90.+y

When a strong electric field is applied to a semiconductor, the steady state of the electrons is determined by specific scattering mechanisms. In a polar semiconductor where scattering is dominated by optical phonons, it is well known that this steady state ceases to exist for a range of electric fields above some critical value.[1,2] Such an effect is related to the Coulomb nature of the electron–polar-optical-phonon scattering. The rate of this scattering is inversely proportional to the square of the momentum change during a scattering event and, thus, decreases for the electrons with high momenta and energies. Above the critical field, the electron momentum and energy gained from the field cannot be relaxed to the lattice when a sufficiently large number of carriers streams into the high-energy states with a relatively low scattering rate. The carriers then accelerate toward higher energies, giving rise to the so-called runaway effect (RAE). In a *bulk-like sample,* the electron runaway is eventually stabilized by such factors as nonparabolicity, transfer to upper valleys, additional scattering mechanisms triggered at high energies, breakdown due to the impact ionization of impurities or across the bandgap, etc. These stabilizing factors have been studied in detail for a number of polar materials.[3–5] In a short sample, however, the runaway can play an important role.

In most publications, the RAE was studied with the use of the Boltzmann transport equation (BTE) under an electron temperature approximation. An exception was made in the seminal paper by Thornber and Feynman.[6] Applying the path-integral technique, Thornber and Feynman derived the dependence of electron energy loss per unit length on the electron drift velocity. The dependence, schematically presented in Fig. 1, has a maximum indicating that no steady state exists above the critical field ε_{th}. For each field $\varepsilon^* < \varepsilon_{th}$, two steady-state velocities can be found. One velocity, denoted as v_s, corresponds to the stable steady state, while the other, denoted as v_u, is the unstable solution. This result enabled Thornber and Feynman suggest that a carrier injected into a sample with a velocity $v_i > v_u$ can be accelerated infinitely (i.e., run away) even in a subthreshold field. Although this *low-field* runaway effect has a fundamental character, it has never been observed nor investigated in detail.

To observe the low-field runaway, the energy of the injected carrier must not exceed the intervalley separation in the conduction band. On the other hand, the relation $v_i > v_u$ has to be satisfied. These two requirements cannot be achieved simultaneously in most of the conventional polar semiconductors. However, the progress in growth, fabrication, and characterization of group-III nitride semiconductors revealed that these wide-gap polar materials can satisfy all the requirements of the low-field runaway. Electron–polar-optical-phonon coupling in group-III nitrides is much stronger than that in III–V compounds.[7] The Fröhlich coupling constants are estimated to be 0.22, 0.41, and 0.74 for InN, GaN, and AlN, respectively (compare to 0.075 for GaAs). Thus, high-field electron transport is mainly determined by the interaction with polar optical phonons. The intervalley separation and breakdown fields in these materials are in the range of 1–2 eV and MV/cm, respectively. In addition, the recent application of the Thornber and Feynman formalism has suggested the possibility of low-field runaway in group-III nitride materials.[8]

In this paper, we calculate the steady-state carrier distribution function in a nanoscale sample operating in the low-field runaway regime. The results demonstrate that a well-developed low-field runaway can be achieved in the wide-gap semiconductors such as group-III nitrides causing spontaneous formation of a two-beam distribution: namely,

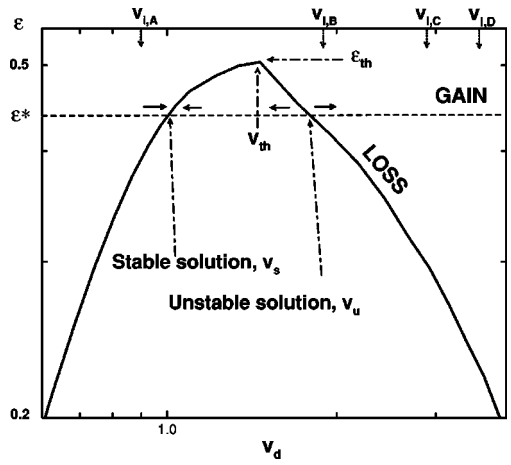

FIG. 1. Energy loss per unit length vs drift velocity. In the dimensionless units, the magnitude of this energy loss rate coincides with the magnitude of field ε. For example, in the steady state an electron experiences energy loss of $W=eFZ$ while traveling a distance Z in an electric field F. When this dimensionless energy loss W/E_{LO} is divided by the dimensionless distance Z/l_O, the resulting expression (i.e., loss per unit length) matches exactly the definition of the dimensionless field ε. Solid arrows indicate expected changes in the average velocity near the points (v_s,ε^*) and (v_u,ε^*).

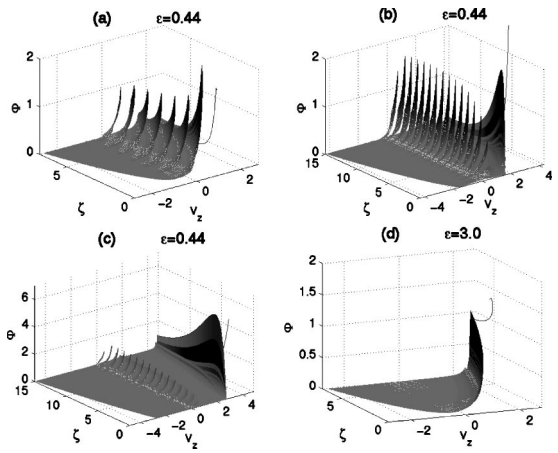

FIG. 2. Distributions of electrons injected with velocities indicated in Fig. 1 by (a,d) $v_{i,A}$; (b) $v_{i,B}$; and (c) $v_{i,C}$.

the splitting of the injected electron beam into two distinct groups of carriers, each with different dynamics. In the first group, the carrier velocity reduces to the thermalized value v_s that corresponds to the stable steady-state velocity in a given subthreshold field. In the second group, the average velocity and kinetic energy increase with the distance. The spontaneous formation of the two-beam electron motion in a short sample is a previously unknown effect which is induced by the instability of the momentum and energy loss–gain balance of hot electrons in subthreshold fields.

To obtain the electron distribution, we solve the BTE analytically using the following assumptions: Electrons are injected into the sample over an emitter barrier with the distribution function $f^{(inj)}(v_\perp,v_z)=f(v_\perp,v_z,z=0)=\delta(v_\perp^2)\delta(v_z-v_i)$, where z is the real-space coordinate and v_z and $v_\perp$ are the parallel and perpendicular projections of the electron velocity with respect to the applied field; the electric field is perpendicular to the barrier heterointerface; the concentration of the injected electrons is small enough to neglect the electron–electron interaction; and emission of the longitudinal optical (LO) phonons is the only scattering mechanism. Since the BTE is linear, the insignificant normalization factor in the distribution function f is omitted. To carry out the analysis, we use the following dimensionless variables: the electron energy $\boldsymbol{\epsilon}$ in units of LO phonon energy $E_{\mathrm{LO}}=\hbar\omega$; electron velocity $\boldsymbol{v}$ in units of $V_O=\sqrt{2E_{\mathrm{LO}}/m}$, where m is the effective mass; electric field ε in units of E_{LO}/el_O, where $l_O=\hbar^2\kappa_0\kappa_\infty/e^2m(\kappa_0-\kappa_\infty)$ with the low-frequency and high-frequency permittivities of the crystal κ_0 and κ_∞; and the distance ζ from the injection point in units of $\varepsilon z/l_O$. In such a representation, the results are dependent only on two dimensionless parameters: the initial electron velocity v_i and the field ε.

Emission of dispersionless LO phonons leads to the electrons descending down the ladder of the energy $\boldsymbol{\epsilon}$: $\boldsymbol{\epsilon}_0=v_i^2$, $\boldsymbol{\epsilon}_1=v_i^2-1,\ldots,\boldsymbol{\epsilon}_s=v_i^2-s$, where s enumerates the stairs of the energy ladder. Then, the distribution function takes the form: $f(v_\perp,v_z,\zeta)=\Sigma_{s=0}\, f_s(v_\perp,v_z,\zeta)=\Sigma_{s=0}\,\delta(v_\perp^2+v_z^2-\zeta-v_i^2+s)\Phi_s(v_\perp,v_z,\zeta)$. The factors Φ_s can be obtained recursively from the BTE.[9] A detailed description of the recursion procedure was published elsewhere.[10] In general, we utilize an approach similar to that previously used for the analysis of high-field RAE.[11]

It is convenient to discuss the results by classifying them in terms of the diagram of Fig. 1. In the model under consideration, the threshold field ε_{th} for the RAE is approximately 0.5 and v_{th} is the velocity corresponding to ε_{th}. We found solutions of the BTE for the subthreshold field $\varepsilon=0.44$ with three different initial velocities: $v_{i,A}=0.9, v_{i,B}=1.9$, and $v_{i,C}=2.9$. The calculated distribution functions are presented in Figs. 2(a)–2(c), respectively. For the carriers injected with $v_{i,A}(<v_{th})$, the functions $\Phi_s(v_z,\zeta)$ nearly repeat themselves at each sublevel $s>1$ and show hot electron accumulation near the band bottom. In this case [Fig. 2(a)], a strongly dissipative (thermalized) transport regime occurs as expected for a subthreshold electric field. The self-repeating Φ_s at different s stairs is in sharp contrast to the case shown in Fig. 2(d), where $\varepsilon\gg\varepsilon_{th}$ and the RAE is well developed. Although the latter distribution is obtained for the same $v_i(=v_{i,A})$, it is characterized by an increase of average electron kinetic energy with distance, focusing of the carrier velocity along the direction of the applied field, and dominant population of the highest-energy stairs.

The distribution depicted in Fig. 2(b) exhibits the presence of both thermalized and runaway carriers. As shown in Fig. 1 by the solid arrows, carriers with a velocity close to v_u can either accelerate or decelerate until they reach the velocity v_s. As a result, a two-beam velocity distribution forms at the same subthreshold field as v_i increases. For the case $v_i=v_{i,B}$, the contribution of high-energy carriers quickly decays with distance, so that thermalized carriers predominate throughout most of the sample. Only a small number of carriers run away, indicating the proximity of $v_{i,B}$ to v_{th}. Nevertheless, due to the presence of the runaway carriers, the

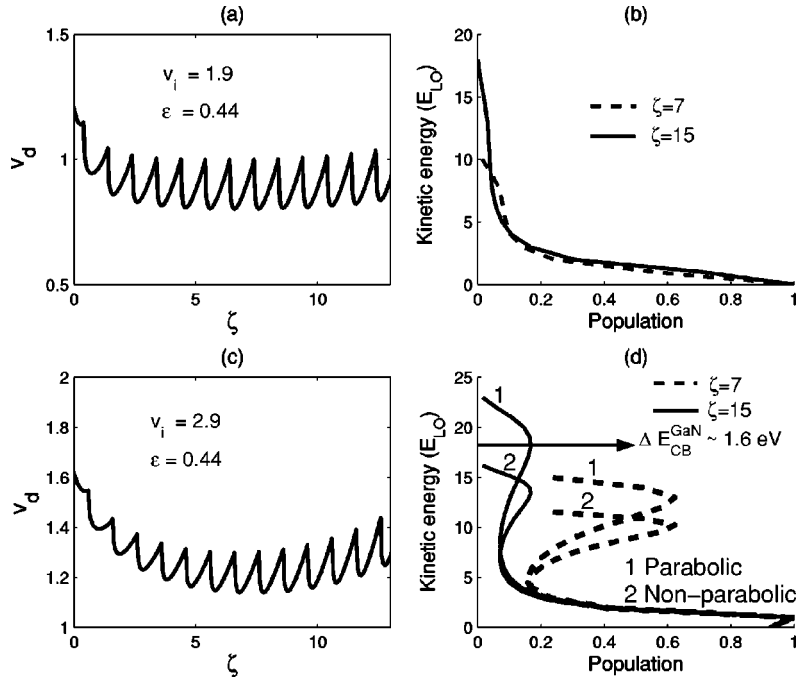

FIG. 3. (a,c) Averaged electron velocities vs distance and (b,d) carrier energy distributions at different distances. Electrons are injected with velocities (a,b) $v_{i,B}$ and (c,d) $v_{i,C}$. In (d), ΔE_{CB} is an estimate of the lowest possible value of intervalley separation in GaN. $\zeta=7$ and $\zeta=15$ correspond to 0.055 and 0.118 μm, respectively.

average drift velocity v_d [shown for this case in Fig. 3(a)] is not as small as that obtained for the electrons injected with $v_{i,A}$. In this case, v_d is not only higher everywhere in the sample, but it also has a tendency to increase with distance. The oscillations in v_d are obviously caused by nearly periodic emission of the phonons typical for thermalized electrons. The presence of high-speed carriers also manifests itself as a weak broadening in the high-energy part of the carrier energy distribution given in Fig. 3(b).

When v_i increases to $v_{i,C}$, the contribution of runaway carriers increases significantly. As shown in Fig. 2(c), the high-energy part of the distribution function decays much more slowly with ζ and becomes comparable to its low-energy counterpart only at $\zeta \geqslant 10$. The drift velocity, when averaged over both electron groups, has a well-pronounced main minimum at $\zeta \approx 8$ [Fig. 3(c)]. The value of this minimum is higher than the drift velocities obtained for the case shown in Fig. 3(a) after the first few oscillations. Moreover, for $\zeta > 8$, a clear increase in v_d is observed. Since the relative contribution of the thermalized carriers is smaller for this case, we also observe a weaker velocity oscillation at $\zeta \lesssim 8$. The increased role of the runaway carriers transforms the high-energy tail into a strongly pronounced additional peak as shown in Fig. 3(d). The shape and position of this peak is distance dependent. As the distance increases, the peak shifts to higher energies and becomes broader.

The development of the high-energy peak continues as v_i increases. The distribution function with the highest injection energy under consideration ($v_{i,D}=3.6$) is shown in Fig. 4. In this distribution, the details of the low-field runaway can be readily seen. Even at $\zeta > 15$, the energy stair $s=1$ remains highly populated with the velocity of most of the carriers focused along the direction of accelerating field. When scattered from this stair, electrons tend to populate the stair $s=2$ rather than to thermalize. The shape of the distributions at stairs 2 and 3 is similar to that for runaway carriers in Fig. 2(d). The redistribution of the carriers between the high-energy stairs occurs more slowly than the growth of their energies leading to the runaway of high-energy carriers. Note that the low-energy part of the distribution is always present regardless of the injection energy. It becomes suppressed only when $\varepsilon > \varepsilon_{th}$.

The group-III nitrides and their alloys are suitable materials for the observation of the subthreshold runaway effect. For GaN, we obtain $m=0.18\,m_0$ (m_0 is the free-electron mass), $\kappa_0=8.9, \kappa_\infty=5.35$, $E_{\mathrm{LO}}=91$ meV,[12,13] $l_O=35$ Å, and

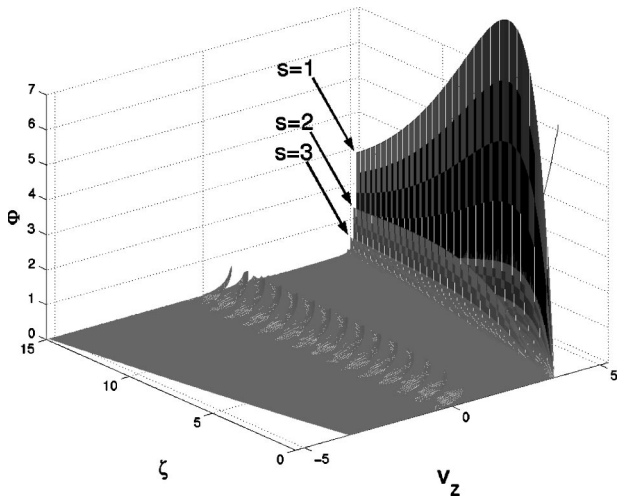

FIG. 4. Distribution of electrons injected with velocity $v_{i,D}$ (see Fig. 1). The applied field ε is 0.44 as in Figs. 2(a)–2(c).

the threshold field $\varepsilon_{th}=130$ kV/cm.[11] Then, the subthreshold field $\varepsilon=0.44$ corresponds to 115 kV/cm [Figs. 2(a)–2(c), 3, and 4] and the field $\varepsilon=3.0$ to 770 kV/cm [Fig. 2(d)]. The velocity V_O in this material is 4×10^7 cm/s; $\zeta=7$ and $\zeta=15$ in Figs. 3(b) and 3(d) correspond to 0.055 and 0.118 μm, respectively. [The dimensionless diagram of Fig. 1 used the estimates made for GaN in Ref. 8.] Thus, the required parameters can be achieved in nanoscale GaN-based heterostructures where the high-energy electrons are injected from the wide-gap AlGaN barrier with an appropriately selected Al composition. Our results are obtained for electrons in a single valley with a parabolic energy dispersion. For the well-developed two-beam distribution presented in Fig. 2(c) and 4, a group of fast electrons occupies the states with quite high energies. Two factors—nonparabolicity and upper valleys—can affect the results. We made corrections for nonparabolicity in GaN by incorporating the standard dependence $v^2=\varepsilon(1+\alpha\varepsilon)$, where α is the nonparabolicity factor,[13] and found that, despite the visible effect, the nonparabolicity does not prevent formation of the two-beam distribution as shown in Fig. 3(d). The other qualitative features of the low-field runaway are also preserved. The energies of the injection barriers used for our calculations as well as the energies of runaway electrons shown in Figs. 2(a)–2(c) do not exceed the energy splitting between the central and satellite valleys in GaN.

Formation of the bimodal distribution by the low-field runaway is qualitatively different from the results obtained in ultrashort devices where the intercontact distance is of the order of the electron mean-free path. In the latter case, a finite number of electrons indeed can move ballistically through the device, which also results in a second peak in the distribution (see, for example, Ref. 14). The energy of this peak obviously corresponds to eU with the applied voltage U. The effect studied in our paper is found for essentially dissipative electron transport with strongly inelastic optical phonon scattering and for distances considerably larger than the mean-free path (i.e., the low-field runaway is not ballistic).

In summary, our results show that the subthreshold runaway can be observed in polar materials with high values of intervalley separation. The effect manifests itself in the spontaneous formation of a two-beam electron distribution and other nontrivial features in the electron dynamics. Low-field runaway is a complex phenomenon characterized by the smooth development of the runaway distribution as the injection energy increases.[15] Due to the transient nature, this phenomenon can occur only in nanoscale structures satisfying a number of stringent conditions. Experimental observation of the low-field runaway[16] can be achieved in group-III nitride-based three-terminal heterostructures similar to the electron-energy spectrometer.[17] This can open opportunities in novel nanoscale devices for high-frequency generation, tunable excitation of intracenter luminescence, and other applications.

This work was supported by the U.S. ARO, the ONR through the MURI program, and CRDF.

*Email: kwk@ncsu.edu

[1] R. Stratton, Proc. R. Soc. London, Ser. A **242**, 355 (1957).
[2] E. M. Conwell, *High Field Transport in Semiconductors* (Academic, New York, 1967).
[3] H. J. Fitting and J. H. Frieman, Phys. Status Solidi A **69**, 349 (1982); H. J. Fitting, J. Boyde, and J. Reinhardt, *ibid.* **81**, 323 (1984).
[4] T. N. Theis *et al.*, Phys. Rev. Lett. **52**, 1445 (1984).
[5] W. Porod and D. K. Ferry, Phys. Rev. Lett. **54**, 1189 (1985).
[6] K. K. Thornber and R. P. Feynman, Phys. Rev. B **1**, 4099 (1970).
[7] D. K. Ferry, Phys. Rev. B **12**, 2361 (1975).
[8] S. M. Komirenko *et al.*, J. Phys.: Condens. Matter **13**, 6233 (2001).
[9] We assume that all carriers are injected with the same v_i. Thus, the factor $\Phi_{s=0}$ takes the form $\Phi_0=\delta(v_z^2-\zeta-v_i^2)\xi(v_z,\zeta,v_i)$. In Figs. 2 and 4, the corresponding functions $\xi(v_z,\zeta,v_i)$ are shown instead of $\Phi_{s=0}$.
[10] S. M. Komirenko *et al.*, *in Advanced Semiconductor Heterostructures: Novel Devices, Potential Device Applications and Basic Properties*, edited by M. A. Stroscio and M. Dutta (World Scientific, Singapore, 2002), pp. 119–143.
[11] S. M. Komirenko *et al.*, Phys. Rev. B **64**, 113207 (2001).
[12] S. J. Pearton *et al.*, J. Appl. Phys. **86**, 1 (1999).
[13] B. E. Foutz *et al.*, Appl. Phys. Lett. **70**, 2843 (1997); B. E. Foutz *et al.*, J. Appl. Phys. **85**, 7727 (1999).
[14] H. U. Baranger and J. W. Wilkins, Phys. Rev. B **30**, 7349 (1984).
[15] We found that the prethreshold RAE for carriers injected with high energies exists also in the case of strong carrier–carrier interaction, when the system can be characterized by the electron temperature. These results will be published elsewhere.
[16] Since optical excitation tends to generate high-energy electrons with an *isotropic* distribution in the momentum space, it is generally inadequate for the LFRAE, which requires a *highly focused* initial velocity distribution. Furthermore, its transient nature necessitates a high degree of local control at the injection point, which is also difficult to achieve in optical experiments. In general, anisotropy of the injected electrons can be characterized by the ratio of transverse and longitudinal velocity components: $V_\perp/V_i=\sqrt{k_BT/E}$, where T and E are the ambient temperature and the energy of injected electrons, respectively. In the nitrides, the injection energy of $E=(1-4)\times E_{\mathrm{LO}}$ is sufficient to provide the condition for a highly focused distribution (i.e., $V_\perp/V_i\ll1$). The injection energy of this magnitude can be readily achieved in the AlGaN/GaN heterostructures.
[17] A. F. J. Levi *et al.*, Phys. Rev. Lett. **55**, 2071 (1985); M. Heiblum *et al.*, *ibid.* **55**, 2200 (1985).